PERGAMON

International Journal of Heat and Mass Transfer 45 (2002) 4871–4879

International Journal of HEAT and MASS TRANSFER

www.elsevier.com/locate/ijhmt

A unified analysis on enhancing single phase convective heat transfer with field synergy principle

W.Q. Tao *, Y.L. He, Q.W. Wang, Z.G. Qu, F.Q. Song

School of Energy and Power Engineering, Xi'an Jiaotong University, Xi'an, Shaanxi 710049, China

Received 7 January 2002

Abstract

Numerical simulations were conducted to reveal the inherent relation between the filed synergy principle and the three existing mechanisms for enhancing single phase convective heat transfer. It is found that the three mechanisms, i.e., the decreasing of thermal boundary layer, the increasing of flow interruption and the increasing of velocity gradient near a solid wall, all lead to the reduction of intersection angle between velocity and temperature gradient. It is also revealed that at low flow speed, the fin attached a tube not only increases heat transfer surface but also greatly improves the synergy between the velocity and the temperature gradient.

1. Introduction

Many techniques have been developed to enhance the heat transfer [1,2]. The passive techniques of enhancing convective heat transfer can be grouped usually into three types of enhanced methods:

(1) Decreasing the thermal boundary layer thickness [3–5]. According to this way, a lot of enhancing surfaces, such as off-set fin in compact heat exchanger, slotted fin in plate fin-and-tube heat exchangers, are adopted in industries.
(2) Increasing the interruption in the fluids [6–8]. Flow interruption is a well-developed technique to enhance convective heat transfer, and all kinds of inserted devices belong to this type [3]. In addition, the louvered fins or plates obliquely positioned to the oncoming flow also serve to interrupt the flow [6,7]. The rib-roughened ducts [8] adopted in the cooling technique for the turbine blade provide another example.
(3) Increasing the velocity gradient near a heat transfer wall. It was found in [9] that by inserting a co-axial tube in a heat transfer tube the heat transfer between the fluid and the outside tube can be appreciably enhanced. Later, in [10] this idea was extended in that the inserted tube was blocked to force all the fluid going through the annulus between the inner tube and the outside tube (Fig. 1). Tests have shown that this is an efficient way for enhancing heat transfer for both laminar and turbulent flow [10]. At the fixed flow rate the insertion may make the velocity gradient near the heat transfer wall larger than that without the insertion, leading to the enhancement of heat transfer.

So far, even for single phase convective heat transfer, no unified theory can reveal the essence of the heat transfer enhancement.

In 1998 Guo and his co-workers proposed a novel concept of enhancing convective heat transfer based on the parabolic fluid flow situation [11,12]. They transformed the convection term into the form of dot product of velocity and temperature gradient, and integrated the energy equation over the thermal boundary layer. They pointed out that by reducing the intersection angle between velocity and temperature gradient, the convective heat transfer can be effectively enhanced. This concept has been extended to elliptic fluid flow and other transport phenomena, and is called field synergy

* Corresponding author.
E-mail address: wqtao@mail.xjtu.edu.cn (W.Q. Tao).

0017-9310/02/$ - see front matter
PII: S0017-9310(02)00173-4

Nomenclature

C	coefficient in Eq. (5)	x, y	Cartesian coordinates (m)
c_p	specific heat capacity ($J\,kg^{-1}\,K^{-1}$)	Γ	diffusion coefficient ($m^2\,s^{-1}$)
H	duct height or transverse distance between plates (m)	δ_t	thermal boundary layer thickness (m)
		η	dynamic viscosity
h	heat transfer coefficient ($W\,m^{-2}\,K^{-1}$)	θ	intersection angle between velocity and temperature gradient (°)
Int	integral, $\int_\Omega \rho c_p(\vec{U}\cdot \mathrm{grad}T)\,dA$ (W)		
L	length (m)	λ	thermal conductivity ($W\,m^{-1}\,K^{-1}$)
n	exponent in Re	ρ	fluid density ($kg\,m^{-3}$)
Nu	Nusselt number	ϕ	general variable
Q	heat transfer rate (W)		
Re	Reynolds number	*Subscripts*	
r	radius (m)	f	fluid
S	source term	in	inlet
T	temperature	m	mean
u, v	velocity component in x- and y-directions	out	outlet
$\vec{U}$	velocity vector	w	wall

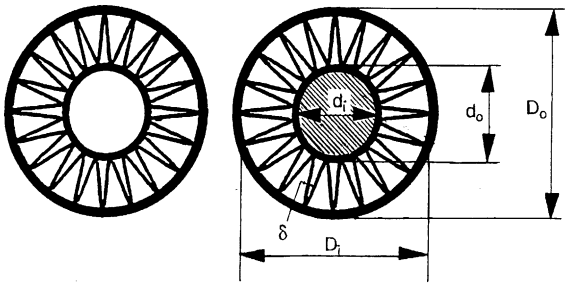

Fig. 1. Center unblocked and blocked tubes with longitudinal fins.

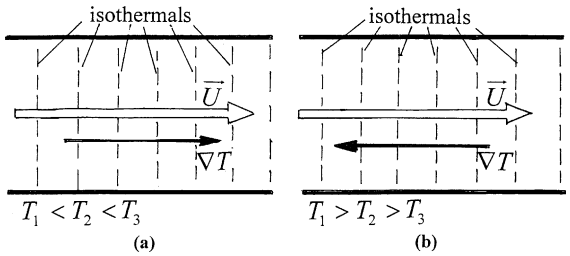

Fig. 2. Ideal case of convective heat transfer—full synergy between velocity and temperature gradient (a) fluid heated, (b) fluid cooled.

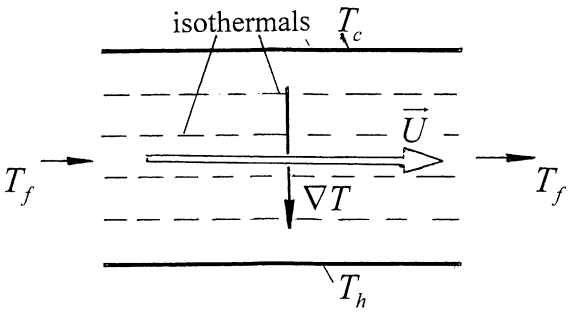

Fig. 3. Non-synergy case of velocity and temperature gradient.

principle [13,14]. The word "synergy" indicates the cooperative characteristics of different forces or actions which exist in a same transport process [15]. For single phase convective heat transfer velocity and temperature gradient are the two vectors which dominate the process. In this paper, discussion will be conducted by numerical methods to show that the above-mentioned three method's for enhancing single phase convective heat transfer can be unified by the field synergy principle, and to provide an interesting example, which shows that the function of fin under low flow speed is to make the velocity and temperature gradient having a better synergy.

We first show two limit cases of convective heat transfer: the full synergy case (Fig. 2) and non-synergy case (Fig. 3). In Fig. 2(a), the directions of velocity and temperature gradient, grad$T$, coincide each other and the fluid is heated along the flow direction; while in Fig. 2(b), the directions of velocity and grad$T$ are opposite, and the fluid is cooled. It is easy to show that for the full synergy case, the heat transfer coefficient is directly proportional to the fluid velocity. For the non-synergy case shown in Fig. 3, the heat transfer from high temperature wall to low temperature wall is simply by conduction, and the fluid motion does not make any contribution for enhancing heat transfer.

2. Numerical demonstrations for the relation between field synergy and the methods for enhancing single phase convective heat transfer

Attention is now turned to revisit the above-mentioned methods for enhancing single phase convective heat transfer from the point of view of field synergy. For this purpose, three numerical examples are adopted. These are: (1) laminar boundary layer flow over a flat plate with constant wall temperature; (2) laminar duct flow within a parallel plate duct with two inserted square cylinders to produce flow interruption; and (3) laminar flow in a tube with an inserted co-axial cylindrical bar. For all the three cases, the solid wall are kept at constant temperature and heat transfer occurs between the surface and the fluid. Numerical method used to predict the heat transfer characteristics is the finite volume approach with SIMPLE algorithm for the coupling of velocity and pressure. All the three numerical examples are of 2-D type, and the flow are assumed to be laminar and in steady state. For simplicity of presentation, following symbols are adopted:

(1) $\mathrm{Int} = \int_{\Omega} \rho c_{\mathrm{p}} (\vec{U} \cdot \mathrm{grad} T)\,\mathrm{d}x\,\mathrm{d}y$
(2) θ_{m} is the average intersection angle between the velocity vector and the temperature gradient in the entire computational domain or in the cross-section studied. If the local value of θ is greater than 90°, its value is taken as $(180 - \theta)$ when added to the summation of the intersection angle.
(3) The symbol h_x stands for the local heat transfer coefficient, and h for the domain averaged value.

The governing equations for the cases (2) and (3) are of elliptic type, for the convenience of coding, however, the first case was also computed by the elliptic equation. All the governing equations can be generalized as follows:

$$\rho c_{\mathrm{p}} \mathrm{div}(\rho \vec{U} \phi) = \Gamma_{\phi} \mathrm{div}(\mathrm{grad}\phi) + S_{\phi} \tag{1}$$

where ϕ stands for the general dependent variables, S_{ϕ} and Γ_{ϕ} are the correspondent source term and diffusion coefficient, respectively, or $\Gamma_{\phi} = \eta$ for velocity and $\Gamma_{\phi} = \lambda$ for temperature. All the thermal physical properties are assumed to be constant. Thus in the Cartesian coordinates the source terms for every dependent variables are zero [15], and for the cylindrical coordinates we have:

$$S_u = 0; \quad S_v = -\eta v / r^2 \tag{2}$$

The boundary conditions for each case will be indicated one by one.

2.1. Reducing the thermal boundary layer

Numerical computations were conducted for air flowing over a plate with constant temperature. The Reynolds number based on the plate length is 600. The computational domain is a rectangular with the length of the plate as the bottom and the height perpendicular to the plate being 1/6 of the length. The inlet distributions are uniform for both velocity and temperature and at the outlet of the computational domain local one-way behavior [16] was assumed. At the top boundary of the computational domain, uniform velocity and temperature condition was assumed. The grid number used was 122×22. The computed average intersection angle of different sections, the related local heat transfer coefficient h_x, and the value of Int are presented in Fig. 4, where only the results in first one third of the longitudinal computational domain are presented, since all the variables are approaching constant in the remaining region. It can be clearly observed that with the increase in thermal boundary layer, the intersection angle between velocity and grad$T$ increased, leading to a worse synergy between velocity and grad$T$. Similar results are obtained for other two Reynolds number cases ($Re = 800$ and 1000), and the results are very similar. For simplicity of presentation, they will not be cited here. This numerical example shows that the decrease of thermal boundary layer is equivalent to the reduction of the intersection angle between velocity and temperature gradient.

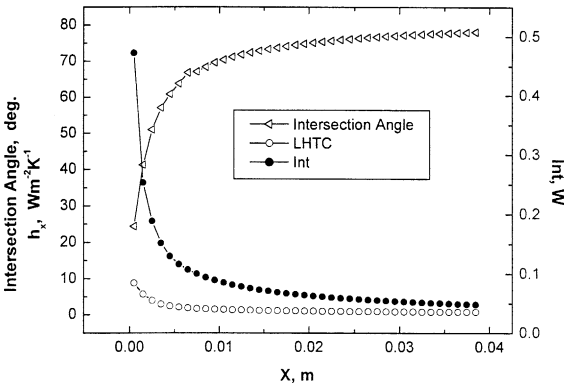

Fig. 4. The distribution of Int, h_x and θ_{m} along flow direction in boundary layer flow.

2.2. Increasing the interruption within fluid

To reveal the inherent relation between the intersection angle and the flow interruption, a parallel plate duct with two square insertions has been chosen as our computational domain (Fig. 5) with the parallel continuous duct without insertion as the reference duct. The duct walls were at constant temperature. The geometric parameters were $L/H = 2$, $h/H = 1/3$, $w/h = 1$, $p/h = 1.35$. A mesh with 53×52 grids was adopted. The periodically fully developed condition was used to deal

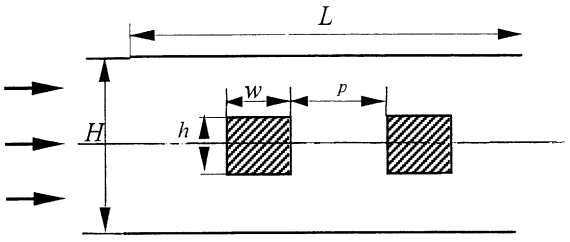

Fig. 5. Parallel plate duct with two inserted square blockages.

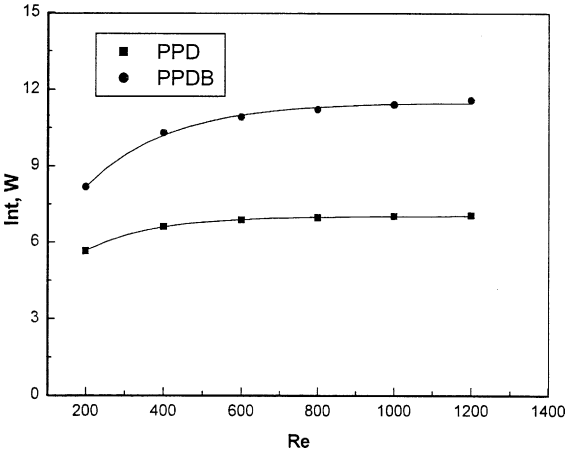

Fig. 6. Int vs. *Re* for parallel plate ducts with or without inserted square blockages.

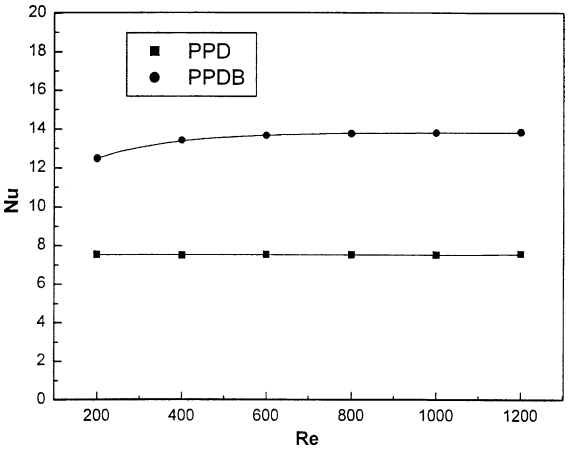

Fig. 7. *Nu* vs. *Re* for parallel plate duct with or without inserted blockages.

with the inlet and outlet boundary conditions. Numerical results of the variation of Int with *Re* is shown in Fig. 6, and that for the Nusselt number in Fig. 7. In these figures, PPD stands for the parallel plate duct, while PPDB means parallel plate duct with blockage. To eliminate other factors' effect, the two inserted blockages were particularly assumed to be thermally isolated from other heat sources, i.e., they did not release thermal energy to or absorb from the fluid, their only function was to introduce interruption within the fluid. And the definition of *Nu* and *Re* are all the same for the two cases:

$$Re = 2Hu_{\mathrm{m}}/v; \quad Nu = 2Hh_{\mathrm{m}}/\lambda \tag{3}$$

where u_{m} is cross-sectional average flow velocity at the inlet of the computational domain, and h_{m} is the average heat transfer coefficient which is determined by:

$$h_{\mathrm{m}} = Q/(2L)/\log\left(\frac{T_{\mathrm{w}} - T_{\mathrm{f,in}}}{T_{\mathrm{w}} - T_{\mathrm{f,out}}}\right) \tag{4}$$

where Q is the total heat transfer rate along the two solid walls, and $T_{\mathrm{f,in}}$ and $T_{\mathrm{f,out}}$ are the fluid temperature at the inlet and outlet of the computational domain.

Two features may be noted from these numerical results. First, both the value of Int and average Nusselt number for the duct with two insertions is much higher than that without insertion. Second, in the lower Reynolds number region, the value of Int decreases with the deceasing in *Re*, while the fully developed Nusselt number of the duct remain the same in the whole range of *Re*. That is, the axial heat conduction within the fluids plays a role. In the higher Reynolds number region, the effect of heat conduction with the fluid can be totally neglected. The average intersection angles of the ducts are presented in Fig. 8, from which the duct with two insertions have a quite significant smaller average intersection angle by around 10°. This demonstrates that the increase of interruption within fluid is actually to decrease the intersection angle between velocity and temperature gradient.

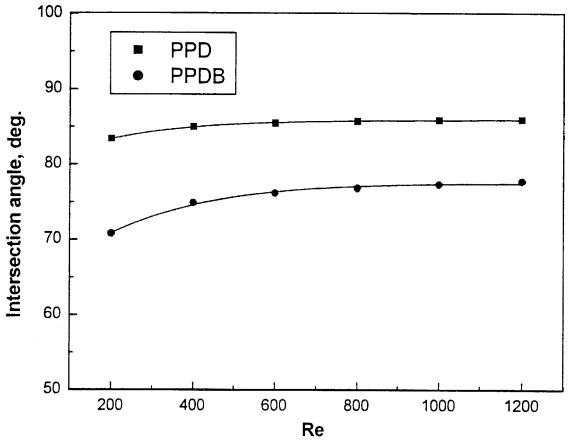

Fig. 8. The variation of average intersection angle with *Re* for parallel plate duct with or without inserted square blockages.

2.3. Increasing the velocity gradient near solid wall

To simulate such an situation, a cylindrical bar was coaxially inserted in a circular tube with constant wall temperature as shown in Fig. 9. A smooth tube without blockage was taken as a reference for comparison. Again the cylindrical bar is isolated from any heat sources and its only function is to increase the velocity gradient along the wall of the outer tube at the same flow rate. And the definitions of *Re* and duct average Nusselt number for the center-blocked tube are the same as those of the tube without blockage, so that the comparison of the numerical results for the two configurations is meaningful. For this case the entrance region was taken as our computational domain. The inlet velocity and temperature distributions were assumed to be constant and the local one-way condition was adopted at the outlet boundary. The geometric parameter were $L_2/L_1 = 0.6$, $L_3/L_1 = 0.2$, $H/D = 0.3$. The grid number used were 52×52. The numerical results of Int vs. *Re* and *Nu* vs. *Re* are presented in Figs. 10 and 11, respectively, where ST represents the smooth tube and TB stands for tube with blockage. The inserted blockage can significantly enhance the heat transfer along the wall of the outside tube. In Fig. 12, the variation of the average intersection angle with Reynolds number is shown, from which the increase in the near-wall velocity gradient in the center-blocked tube also leads to the decrease in the intersection angle between the velocity and the temperature gradient.

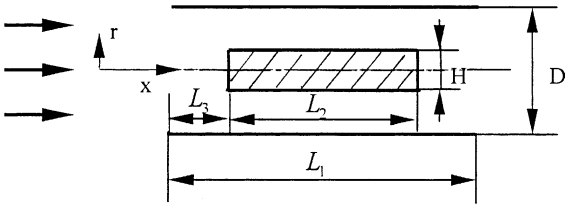

Fig. 9. Circular tube with a coaxially inserted cylindrical bar.

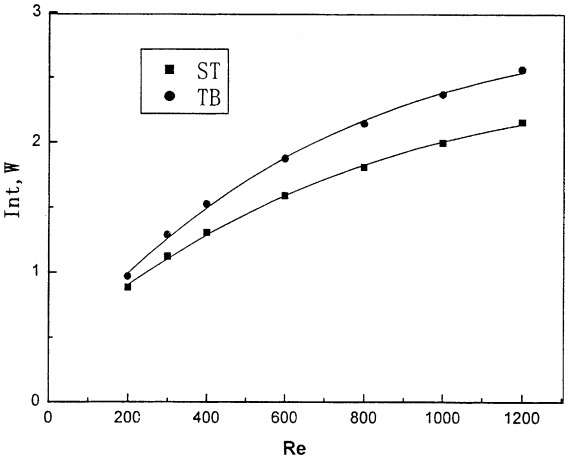

Fig. 10. Int vs. *Re* for tube with a co-axial cylindrical bar.

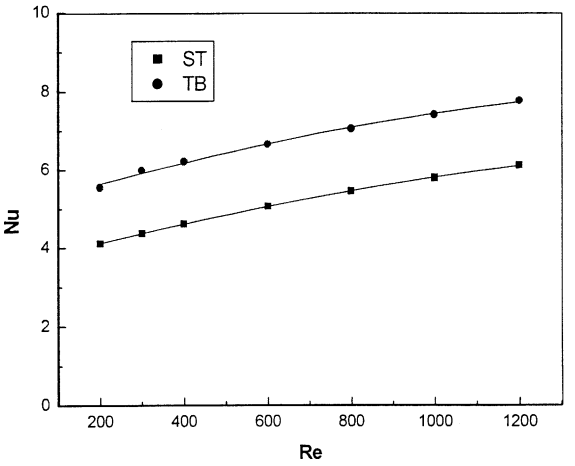

Fig. 11. *Nu* vs. *Re* for tube with a co-axial cylindrical bar.

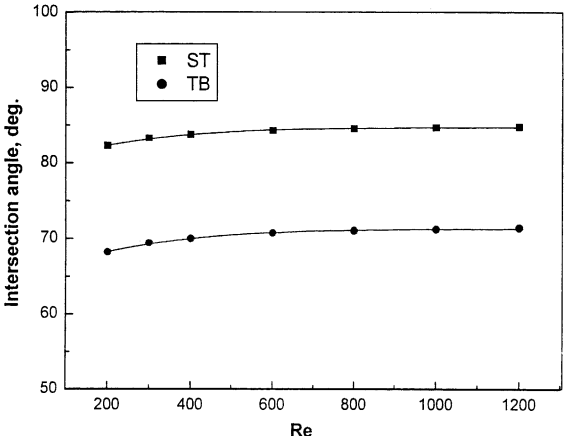

Fig. 12. The variation of average intersection angle with *Re* for tube with co-axial cylindrical bar.

The field synergy principle can reveal the essence common to the above three cases (Sections 2.1–2.3), i.e., decrease the intersection angle between the velocity field and the temperature gradient enhance the single phase convective heat transfer.

3. The role of fin at low fluid speed

For the single phase convective heat transfer, fins, or extended surfaces, are usually considered as being a way to increase the heat transfer surfaces. We found that at low speed of flow velocity, the fin itself can improve the synergy between velocity and temperature. Within the authors' knowledge, this has never been discovered in the literature. Following is our numerical illustration.

The flow and heat transfer across a single circular cylinder with rectangular fins, shown in Fig. 13, was taken as the object for numerical study. The fin pitch was taken as 5 mm. To numerically simulate the flow fields around the cylinder between two adjacent fins three-dimensional body fitted coordinates has been adopted. The uniform inlet condition was adopted, and for the exit boundary condition the local one-way methods was used. The tube wall was kept at constant temperature. For simplicity the fin surface temperature was assumed to be equal to tube wall temperature. The flow across single cylinder was also simulated for comparison. Numerical results of isothermals and velocity vectors for flow over single tube with $U = 0.02$ m/s are presented in Fig. 14, from which over most part of the computational domain, the velocity and the local temperature gradient are nearly perpendicular each other, leading to a large intersection angle. The intersection angle distribution is provided in Fig. 15. The average intersection angle of the whole domain is 61.7° for this case.

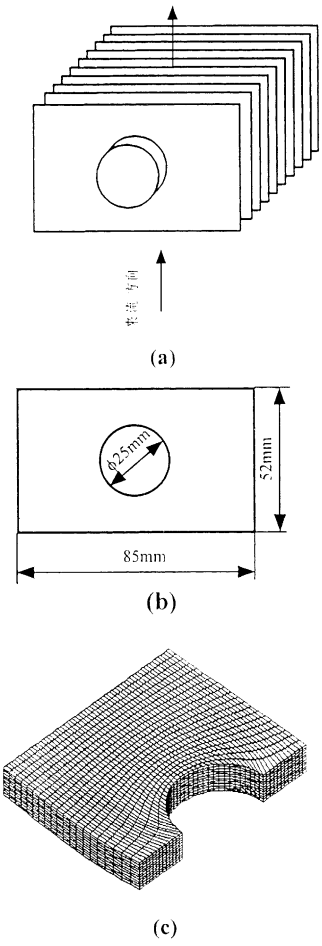

Fig. 13. Flow across single finned tube and computational domain (a) flow over finned tube, (b) fin dimensions, (c) grid system.

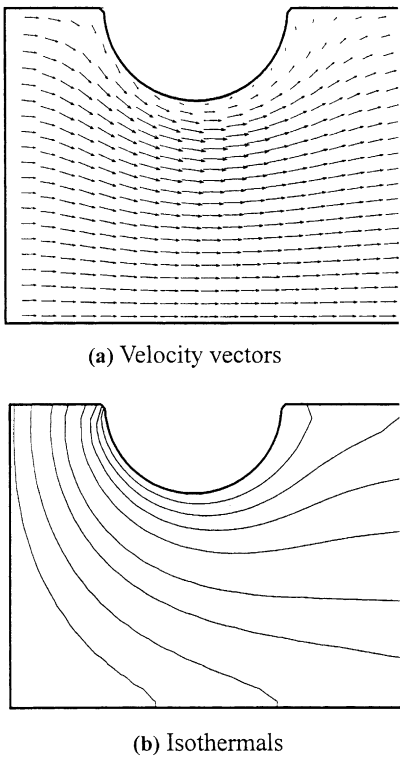

Fig. 14. Numerical results of velocity vectors and isothermals ($U = 0.02$ m/s).

Attention is now turned to the finned tube. At the oncoming flow velocity = 0.06 m/s, the fluid isothermals and the flow velocity at the middle plane between two adjacent fin surfaces are presented in Fig. 16. It can be clearly observed that the attachment of fin to the tube surface greatly changes the orientation of the tempera-

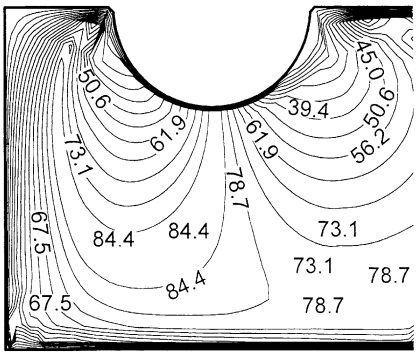

Fig. 15. Intersection angle distribution for flow over single tube ($U = 0.02$ m/s).

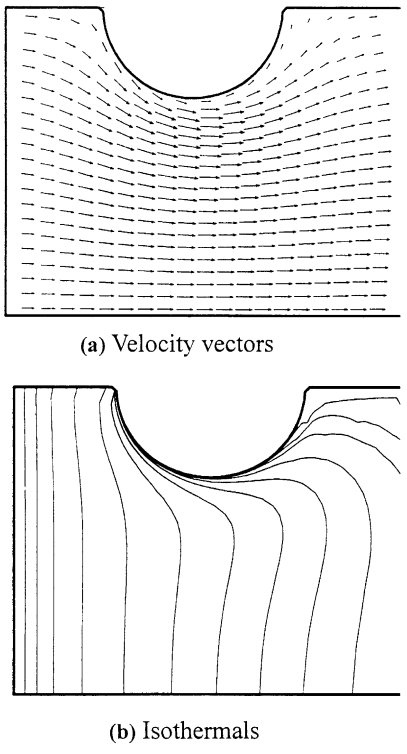

Fig. 16. Velocity vectors and isothermals for flow over finned tube ($U = 0.06$ m/s).

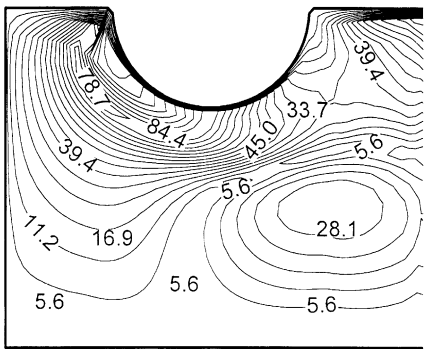

Fig. 17. Intersection angle distribution of flow over finned tube ($U = 0.06$ m/s).

ture isothermal, making the velocity and temperature gradient being in good synergy, with intersection angle distribution shown in Fig. 17, and the average intersection angle is now reduced to 23.6°. Computational results further reveal that in the region of very low velocity (for the case studied, the oncoming flow velocity less than 0.08 m/s), the average finned tube heat transfer coefficient is almost varies linearly with the flow velocity, while in the relatively high velocity region the increase of velocity does not have such efficient enhancement result.

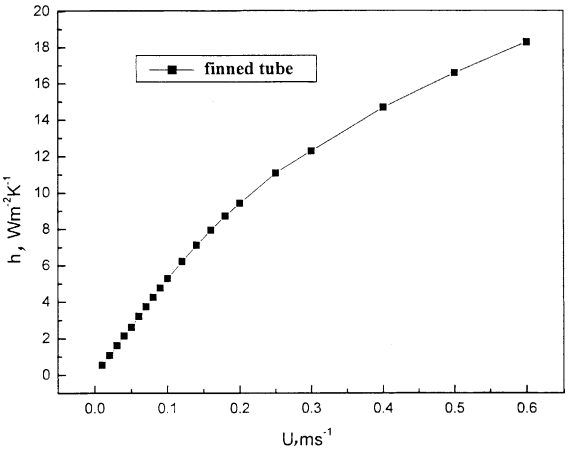

Fig. 18. The variation of heat transfer coefficient with oncoming flow velocity.

Fig. 18 provides such information. This means that with the increase in flow velocity the synergy between velocity and temperature gradient become worse, basically caused by the occurrence of flow separation behind the cylinder. Figure 19 presents the velocity and temperature fields for flow at a higher oncoming flow rate

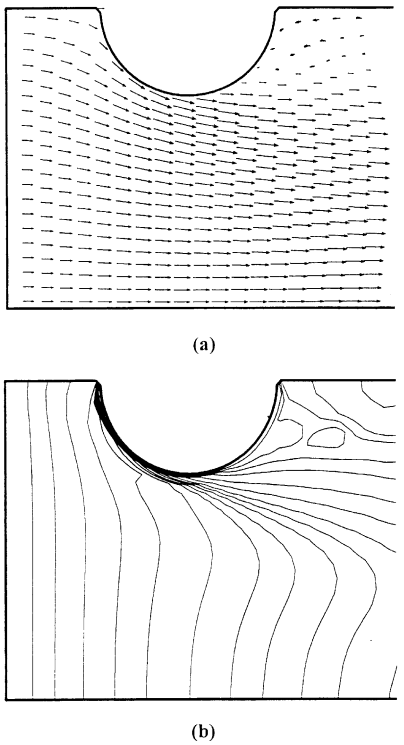

Fig. 19. Velocity and isothermal distributions of flow across finned tube at higher flow rate ($U = 0.6$ m/s). (a) Velocity vector. (b) Isothermals.

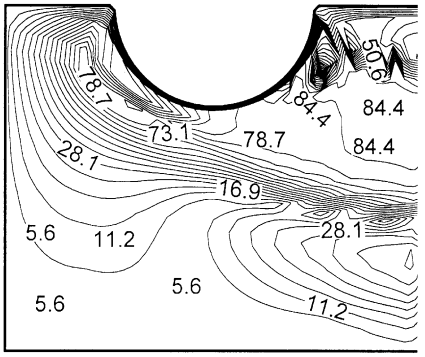

Fig. 20. Intersection angle distribution for flow across finned tube ($U = 0.6$ m/s).

Table 1
Values of c and n in Eq. (5)

Re	C	n
10–100	0.0348	0.9982
100–200	0.0556	0.8991
200–400	0.1638	0.6986
400–600	0.3620	0.5660

($U = 0.8$ m/s). It can be seen that the occurrence of the vortex behind the tube re-orients the isothermals such that the intersection angles in that region become larger (Fig. 20), thus deteriorating the heat transfer in some extent.

Correlating the numerical results via

$$Nu = CRe^n \tag{5}$$

we obtained the value of C and n, as listed in Table 1. For $Re \leqslant 100$ (corresponding to $U \leqslant 0.8$ m/s for the case studied), the exponent in Re nearly equals 1, giving a strong support to the field synergy principle. This reveals that at low flow velocity apart from the increase in heat transfer surface, the fin can also greatly improve the synergy between velocity and temperature gradient.

4. Conclusions

Numerical analyses have been conducted to reveal the inherent relationship between the available single phase convective heat transfer enhancement and the synergy between velocity and temperature gradient. It turns out that the common essence of the three existing enhanced methods is the same decreasing the intersection angle between velocity and the temperature gradient, or, to making the velocity and temperature gradient in a better synergy.

Analysis for the heat transfer across single cylinder with or without fins clearly show that the at low flow velocity, the fin can significantly improve the synergy between velocity and temperature gradient, leading to linear variation trend between heat transfer coefficient and velocity.

Acknowledgements

This work was supported by the National Fundament R&D Project of China (grant number 2000026303). The authors are grateful to Professor Guo, Z.Y. for his help during the study.

References

[1] A.E. Bergles, Heat transfer enhancement—the maturing of second generation heat transfer technology, Heat Transfer Eng. 18 (1) (1997) 47–55.
[2] A.E. Bergles, Enhanced heat transfer: endless frontier, or mature and routine? Enhanced Heat Transfer 6 (1999) 79–88.
[3] R.L. Webb, Principle of Heat Transfer, Hemisphere Pub. Co, New York, 1955.
[4] F.P. Incropera, D.P. DeWitt, Introduction to Heat Transfer, third ed., John Wiley and Sons, New York, 1996, p. 396.
[5] Y.A. Cengel, Heat Transfer, A Practical Approach, WCB McGraw Hill, Bostob, 1998, p. 378.
[6] Y.N. Lee, Heat transfer and pressure drop characteristics of an array of plates aligned at angles to the flow in a rectangle duct, Int. J. Heat Mass Transfer 2 (1986) 1553–1563.
[7] L.B. Wang, G.D. Jiang, Q.W. Tao, H. Ozoe, Numerical simulation on heat transfer and fluid flow characteristics of arrays with non-uniform plate length positioned obliquely to the flow direction, ASME J. Heat Transfer 120 (1998) 991–998.
[8] L.B. Wang, W.Q. Tao, Q.W. Wang, T.T. Wong, Experimental study of developing turbulent flow and heat transfer in ribbed convergent/divergent square ducts, Int. J. Heat Fluid Flow, 22 (2001) 603–613.
[9] W.S. Fu, C.C. Tseng, C.S. Huang, Experimental study of the heat transfer enhancement of an outer tube with an inner-tube insertion, Int. J. Heat Mass Transfer 38 (1995) 3443–3454.
[10] B. Yu, J.H. Nie, Q.W. Wang, W.Q. Tao, Experimental study on the pressure drop and heat transfer characteristics of tubes with internal wave-like longitudinal fins, Heat Mass Transfer 35 (1) (1999) 65–73.
[11] Z.Y. Guo, D.Y. Li, B.X. Wang, A novel concept for convective heat transfer enhancement, Int. J. Heat Mass Transfer 41 (1998) 2221–2225.
[12] S. Wang, Z.X. Li, Z.Y. Guo, Novel concept and device of heat transfer augmentation, in: Proceedings of 11th IHTC, vol. 5, 1998, pp. 405–408.
[13] W.Q. Tao, Z.Y. Guo, B.X. Wang, Field synergy principle for enhancing convective heat transfer—its extension and numerical verifications. Int. J. Heat Mass Transfer, in press.

[14] Y.L. He, Theoretical and experimental investigations on the performance improvements of split-stirling cryocooler and pulse tube refrigerator. School of Energy & Power Engineering, Xi'an Jiaotong University, Xi'an, China, 2002, Ph.D. thesis.

[15] D.B. Guralnik (Ed.), WEBSTER'S New World Dictionary of the American Language, Second College Edition, William Collins Publishers, Inc, Cleveland, 1979, p. 1444.

[16] W.Q. Tao, in: Numerical Heat Transfer, second ed., Xi'an Jiaotong University Press, Xi'an, 2001 (in Chinese).